CLASSIFICATION OF DETAILED FLOODPLAIN VEGETATION LAND COVER BY COMBINING SUB-PIXEL AND OBJECT-BASED IMAGE ANALYSIS IN THE LOWER AMAZONIAN FLOODPLAIN

A Technical Paper

Presented to

the Faculty of Natural Sciences and Mathematics

University of Denver

In Partial Fulfillment

of the Requirements for the Degree

Master of Science in Geographic Information Science

---

by

Katrina E. Waechter

August 5, 2015

Advisor: Dr. Rebecca L. Powell

Table of Contents

Table of Tables and Figures

ABSTRACT

In the face of increased land use pressures and climate change, floodplains in the Lower Amazon region are increasingly vulnerable. A detailed land-cover map of the floodplain is needed to assess the impacts of increased land use pressures. Assessing land use and land-cover changes requires accurate representation of important land covers, a persistent challenge in the complex and dynamic environment of the Amazon River floodplains. This study maps detailed floodplain vegetation for a 663 square kilometer area of the Lower Amazon River floodplain using Quickbird 2 scenes (28 October, 2005) and a cotemporaneous Landsat 5 TM scene (29 October, 2005). Sub-pixel analysis data products are incorporated into a hierarchical object-based classification of (semi-) natural floodplain vegetation, as defined by the United Nations Food and Agricultural Organization's Land-cover classification System (DiGregorio 2005). Within (semi-)natural floodplain vegetation, the land-cover classes of interest include forest, open woodland, closed shrubland, and open shrubland. As part of the detailed floodplain vegetation classification, we mapped the extent of woody vegetation (86% overall accuracy). Within areas mapped as woody vegetation, we classified the amount of vegetation cover (94% overall accuracy) and dominant woody vegetation lifeforms (90% overall accuracy). The vegetation cover and dominant woody lifeform classifications utilize the spectral information and spatial relationships between meaningful image objects. The resulting detailed floodplain vegetation classification reveals a dominance of closed and open shrubs within a complex distribution of vegetation structure and dominant lifeforms. Woody vegetation is distributed as 18% (29,879 m^2) of forest, 13% (23,448 m^2) of open woodland, 20% (34,616 m^2) of closed shrub, 26% (46,291 m^2) of open shrub, and 23% (40,490 m^2) of herbaceous cover. Improved identification of detailed floodplain vegetation provides a basis for studying localized land-cover changes, improved estimates of ecological contributions for specific floodplain habitats, and evaluating the impacts of household land use decisions.

1. Introduction

The distribution of vegetation within the floodplains of the Amazon River and its major tributaries constitutes the ecological and economic importance of its ecosystems (Junk, 1997). A variety of plant communities ranging from aquatic to terrestrial and algal to herbaceous to woody are found within the floodplains. Variability in local flood regimes is related to distribution of vegetation (Ferreira-Ferriera et al., 2015), which creates a gradient of habitats within each floodplain. Floodplain habitats are situated along a gradient of permanently aquatic to permanently terrestrial conditions; the permanent aquatic habitats of the Amazon floodplains are river channels and perennial floodplain lakes while permanently terrestrial habitats are sediment depositions above the highest flood extent that form the uplands. The floodplains occupy a smaller total area compared to the upland forests, but their contributions to biodiversity and ecosystem services are greater than the upland forests (Martinez and LeToan, 2007).

Dominant economic activities in the area include commercial fishing and livestock grazing, the impacts of which cause significant habitat degradation (McGrath et al., 2007). Historically, the floodplain forests were selectively logged for timber and fire wood (Smith, 1999). With the jute boom of the mid-twentieth century, floodplain forests were cut down to cultivate jute (WinklerPrins, 2006). While forest cover is recovering in some areas, the expansion of cattle and water buffalo ranching is causing pasture conversion to expand at an increasing rate (Sheikh et al. 2006; Goulding et al. 1996). Forested areas of the Lower Amazon floodplains have decreased 13% between the 1970s and 2008 while other land covers, such as non-forest vegetation and bare soil, have increased (Reno et al., 2011).

In a complex and dynamic environment such as the Lower Amazon floodplain, accurate and consistent land-cover mapping is challenging. Optical sensors have been used to map floodplain vegetation in the Amazon (Mertes et al., 1995; Novo & Shimabukuro, 1997; Reno et al., 2011), but are limited by clouds or smoke that frequently obscure the ground and the mismatch between image resolution and geographic feature size. Additionally, the level of detail in floodplain vegetation mapping is frequently nominal, often describing land use or using non-diagnostic criteria to define land-cover classes. Accurate and consistent land-cover mapping in this environment is critical for several reasons, including biogeochemical applications, effective management of natural resources related to fishing and ranching, land use impacts, and accounting of landscape heterogeneity. The combined effect of projected climatic changes and increasing anthropogenic pressures could lead to significant changes in ecosystem dynamics in the floodplain. Landscape heterogeneity needs to be fully accounted for to better forecast impacts on ecosystem processes in the Amazon region (Silva, 2015). We present here our approach for mapping floodplain vegetation by two systematic criteria (vegetation cover, vegetation type) at 30-meter resolution. This study produces a high-resolution floodplain vegetation map and addresses questions pertinent to land-cover mapping at high resolution using optical sensors exclusively, such as:

- Given the limitations of using optical imagery in a cloud-covered region, what information can be extracted from multiple optical data sources? How can relevant information be preserved between differing spatial scales?

- How can pixel- and object-based image analyses contribute different and significant information in land-cover classification?

2. Background

2.1 Previous Work

Within the Lower Amazon region, vegetation classification studies (excluding aquatic herbaceous focused) used optical imagery to create cloud-free mosaics (Novo and Shimabukuro 1997), test processing algorithms and utility of sensor capabilities

(Adams et al. 1995; Silva et al. 2007), measure vegetation cover types (Wittmann et al. 2002b; Brondizio et al. 1996), monitor changes in vegetation patterns not caused by landscape degradation or forest succession (Peixoto et al. 2009), detect seasonal patterns of leaf phenology (Hess et al. 2009), study the relationship between hydrological features and vegetative cover (Mertes et al. 1995; Wittmann et al. 2002a), and changes through time between basic land-cover classes (e.g., forest, non-forest, deforestation, water; Reno et al., 2011). A major constraint of optical remote sensing in the Amazon region is the near constant cloud cover, creating a bias of existing optical imagery in that most of the usable scenes were collected during the dry season (Roberts et al., 2003) and have poor temporal resolution between usable images (Melack and Hess 2009). However, optical imagery is still available and could be leveraged for additional information, particularly with the availability of very high resolution optical imagery as well as image archives prior to the 1990s.

The dry season bias has been addressed by use of synthetic aperture radar (SAR) imagery. SAR sensors can penetrate cloud cover and are better equipped to detect flooding beneath vegetation as well as map wetlands and associated land covers (Barbosa, 2000). Several studies have addressed vegetation mapping as a function of flood water extent (Costa 2004) and passive and active microwave systems have been employed to detect the presence of surface water underneath vegetation (Hess et al. 1990; Hess et al. 2003; Martinez and Le Toan 2007). Costa (2004) determined that semi-aquatic vegetation, tree-like aquatic plants, and shrub-like trees colonize flooded regions for at least 300 days a year, secondary colonizers (well-developed floodplain forest) cover regions inundated approximately 150 days a year, and floodplain climax forest colonizes regions inundated for approximately 60 days a year. Similarly and upstream from the current study area, Ferriera-Ferreira et al. (2015) were able to map flooding extent and vegetation zone, showing that the relationship between inundation and vegetation zonation should be refined locally. More related to the current study, a previous vegetation map covering the Lower Amazon River floodplain mapped vegetation type or physiognomy and inundation (e.g., bare or herbaceous and nonflooded, herbaceous and flooded, shrub and nonflooded, shrub and flooded, woodland and flooded, forest and nonflooded, forest and flooded) using normalized dual-season synthetic aperture radar images from 1996 at 100-meter scale (Hess et al., 2003), which is the most detailed, systematic floodplain vegetation map in the current study area to date. This study accurately mapped the floodplain habitats at high resolution but found that low accuracies in mapping herbaceous vegetation and woodland vegetation resulted from coinciding backscattering responses with forest vegetation.

These previous studies confidently classify forest, but account for non-forest vegetation less accurately. Forest is more consistently and accurately classified because of its distinctive spectral response and regular structure. Forest and bare ground comprise the ends of a dichotomous spectrum between peak vegetation and vegetation absence. Vegetation types other than forest (including herbaceous, shrubs, and woodlands) typically have more subtle compositional differences (within woody and herbaceous sub-groups), highly variable statures, exhibit difficult to track seasonal

changes in stands, and comprise small features of interest. Non-forest vegetation is also difficult to systematically define, causing confusion and inability to compare vegetation classification studies between different time periods and areas within the Amazon region.

2.2 Classification Scheme

Based on the need to generate a comprehensive, clear and systematic description of land-cover classes within the study area, we choose to use the United Nations Food and Agriculture Organization's Land-cover classification System (DiGregorio 2005) as the classification scheme. The Land-cover classification System, referred to here as LCCS, is a two phase *a priori* classification system that uses standardized criteria to describe the detail of land-cover classes with understandable class names. Its output is a comprehensive characterization of land cover, regardless of mapping scale, data collection method, or geographic location.

In this approach, a land-cover class is defined by the combination of a set of independent diagnostic attributes, which retain Boolean formula of the attributes used and unique map codes. Class boundaries are defined by either the different amount of attribute(s) or the different types of attribute(s). Thus, the class is defined as the set of attributes used rather than a presupposed class name or legend. Table 1 reconciles the LCCS land-cover classes with more common names.

Boolean formula	**Legend name**	**Standard class name**
A24A3A12	Closed, tree	Forest
A24A3A13	Open, tree	Woodland
A24A4A12	Closed, shrub	Closed Shrub
A24A4A13	Open, shrub	Open Shrub
A24A2A17	Sparse, herbaceous	Sparse Vegetation (woody vegetation 10-4% of cover)
A24A2A18	Very sparse, herbaceous	Sparse Vegetation (woody vegetation 4-1% of cover)

Table 1: LCCS land-cover classes of interest

The first phase of LCCS uses three dichotomous decision points using presence of vegetation, edaphic condition, and artificiality of cover to select one of eight major land-cover classes. For this study, Natural and Semi-Natural Aquatic or Regularly Flooded Vegetation (Boolean code: A24) is the only dichotomous land-cover class of interest. This class includes all non-cultivated vegetated areas (herbaceous and woody) within the floodplain. In this study, *cover* and *lifeform* are the attributes used to define land-cover classes of interest as part of the modular-hierarchical phase of LCCS. Table 2 recaps the modular-hierarchical phase land-cover classifiers used by this study.

- Cover can be considered as the presence of a particular area of the ground, substrate or water surface covered by a layer of plants considered at the

greatest horizontal perimeter level of each plant in the layer (Eiten, 1968). Distinctions are made between *Closed* (>60-70%), *Open* (between 60-70% and 10-20%) and *Sparse* (<10-20% but >1%) cover. A closed cover (Boolean code: A12) composed of Trees or Shrubs has crowns interlocking, touching or very slightly separated. The crowns can form an even or uneven closed canopy layer. An open cover (Boolean code: A13) composed of Trees or Shrubs has the plants standing rather close together and may appear to grow continuously from a distance (Kuechler and Zonnevled, 1988). The distance between two plant perimeters equals the mean radius of a crown. A sparse cover (Boolean code: A17 or A18) composed of Trees or Shrubs has great variability in the horizontal character of vegetation and may be associated with another lifeform of great cover continuity, like herbaceous vegetation. The distance between two perimeters of a lifeform is more than twice the average perimeter distance (Eiten, 1968).

- Lifeform of a plant is defined by its physiognomic aspect. This is the case when Woody plants, which are sub-divided into Trees and Shrubs, are distinguished from Herbaceous plants, which are subdivided into Forbs and Graminoids, and Lichens/Mosses. According to (Ford-Robertson, 1971), a tree (Boolean code: A3) is defined as a woody perennial plant with a single, well-defined stem carrying a more-or-less-defined crown and being at least 3 meters tall while shrubs (Boolean code: A4) are woody perennial plants with persistent woody stems and without any defined main stem, being less than 5 meters tall. The growth habit can be erect, spreading or prostrate. Plants without persistent stem or shoots above ground and lacking definite firm structure are defined as herbaceous (Scoggan, 1978). Discernment of Forbs and Graminoids is beyond the scope of this study, so herbaceous description (Boolean code: A2) is used in the absence of woody vegetation and presence of vegetation according to the sub-condition of cover rule. This rule holds that if a lifeform is sparse, then the dominance of an area goes to another lifeform that has the highest closed or open cover (DiGregorio 2005).

Classifier	Meaning	Classifier options	Criteria
Cover	Horizontal extent of most prominent plant layer; (woody vegetation only in this case)	Closed Open Sparse	>70% extent 20-69% extent <20% extent
Lifeform	Vegetation body form at maturity; includes sub-types of woody and non-woody plants	Shrub Tree Herbaceous	Woody, <3 m tall Woody, >5 m tall Non-woody+

Table 2: Modular-hierarhical phase classifiers for (Semi-)Natural Regularly Flooded Vegetation (A24)

In this study, differences in land cover, which is defined as the biophysical state of Earth's surface and immediate subsurface (including biota, soil, topography, surface water and ground water, and human structures, Turner et al., 1995), are mostly subtle. Each type of land cover may possess unique materials or surface properties, but the similarity between materials and their relative quantities in the study area makes these

classes difficult to discern. Land-cover mapping needs to consider what phenomena may be influencing the image signal: the surface structure may influence the spectral response as much as the intraclass variability (Herold et al., 2006). Land-cover mapping requires consideration of the intraclass variability and spectral separability. Within remote sensing, it has become clear that mapping detailed land-cover classes from spectral information alone may be limited. Additional information, such as spatial, textural, and contextual information, is usually required to have a successful land-cover classification in areas with difficult to discern land cover types (Weng, 2012).

2.3 Scene Models

No single data source exists that contains sufficient spectral, spatial, textural, and contextual information to satisfy land-cover mapping needs. The best way to maximize information is use of multiple data sources. We hypothesize that sufficient information can be extracted from optical data sources that follow different scene models to allow for a 30-meter resolution vegetation land cover map of the Lower Amazon floodplain. Another significant question for this study is if we can accurately map detailed land cover without relying on water stage, particularly since increasingly variable flood regimes are becoming more common (IPCC, 2007). This study uses information gleaned from H-resolution and L-resolution scene models, as described in Strahler, Woodcock, & Smith (1986), in a hierarchical object-based classification.

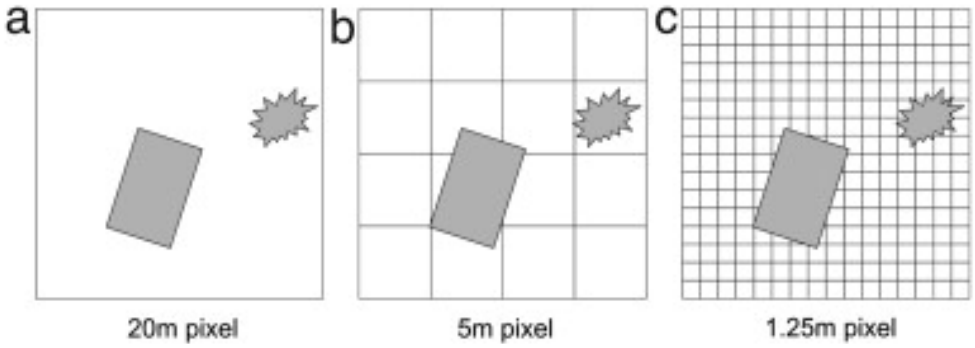

Figure 1: Relationship between objects of interest and spatial resolution: (a) low resolution: pixels are significantly larger than objects, sub-pixel techniques are needed. (b) medium resolution: pixels and objects are of the same order, pixel-by-pixel techniques are appropriate. (c) high resolution: pixels are smaller than the object, regionalization of pixels into groups of pixels and objects is needed. After Blaschke's (2010) Figure 1.

In digital images, a pixel contains both H- and L-resolution information, each of which can be used for image analysis (Hay et al., 2001). The size of the scene objects rather than the size of a pixel relative to the scene is what determines whether there is an H- or L-resolution situation (Blaschke et al., 2014).Sub-pixel refers to low spatial resolution (L-resolution scene model), which occurs when a feature of interest is significantly smaller than the pixel resolution as shown in Figure 1a. The fundamental concept behind sub-pixel classification holds that the spectral reflectance of pixels in medium or coarse resolution imagery can be used to quantify the percent distribution of

different land covers or constituent materials (Anser and Heidebrecht, 2002). Sub-pixel classification is better suited to capture spectral differences from larger geographic features rather than a particular target (Weng and Hu, 2008). Per-pixel refers to medium to low spatial resolution (neither H-resolution or L-resolution scene models), which occurs when an feature of interest is equivalent in size to pixel resolution, similar to Figure 1b. In both cases of low- and medium-resolution models, the spectral response of a "pure" class or material is mixed with the spectral response of other classes or materials. A limitation of the pixel-based approach (for low and medium spatial resolution models) is that it ignores the spatial information and groupings of pixels that need to be considered together as an object (Benz et al., 2004). Situations of high spatial resolution (H-resolution scene model), which occurs when a feature of interest is significantly larger than the pixel resolution as shown in Figure 1c, are the only scene model to allow for the use of spatial and contextual information in an object-based approach (Blaschke, 2010). This model treats features of interest as discrete objects rather than continuous fields and is characterized by the detection of the spatial arrangement of objects (Strahler, Woodcock, & Smith, 1986). Finer resolution results in higher level of detail and increase in spectral heterogeneity, which can lead to lower classification accuracy in complex heterogeneous environments (Rocchini, 2007). Within the vegetation classification studies in the Amazonian floodplains, all three scene models have been and are commonly used depending on the objective of the research. To date, we are not aware of the use of both low- and high-resolution scene models in a vegetation classification in the Amazonian floodplains.

Object-based image analysis (OBIA) is an increasingly popular (Blaschke et al., 2014) and effective approach to classifying high resolution data. Object-based image analysis builds on the process of image segmentation to treat groups of pixels as objects followed by classification of the pixel groups. Taking an object oriented approach is best in cases with high resolution data, similar to Figure 1c, as well as a platform for integration of different data. Objects are regions which are generated by one or more criteria of homogeneity in one or more dimensions (Blaschke 1995). Objects can have additional spectral information compared to single pixels (e.g., mean values per band, median values, minimum and maximum values, mean ratios, variance, etc.) as well as spatial information for segments (e.g., area, length, distance to nearest (sub-)object, neighbor count, etc.; Myint et al., 2011). According to Hay and Castilla (2008), there are four primary advantages to an object-oriented approach. First, multiple scales are used in OBIA, which allows for multiple, related levels of segmentation and image objects. In pixel-based image analysis, the pixel is assumed to cover an area meaningful at the landscape level when it is often not the case. Results from object-based image analyses more closely approach the goal of real world feature extraction (Fernandez-Manso et al., 2005). Second, the spatial relationships with adjacent, nearby, super- or sub-objects provide additional information at various complexity levels. Hierarchical object-based classifications yield increasingly accurate results in heterogeneous environments (Addink et al., 2007; Burnett and Blaschke, 2003; Hall et al., 2004; Zhou and Troy, 2008). Third, OBIA acts as an information filter for non-relevant information while assimilating other pieces of information into a single object. Because of the volume of data within high and very high resolution imagery like

Quickbird, this characteristic of OBIA helps to decrease processing time. Fourth, OBIA allows for use of fuzzy logic, which is ideal for capturing areas of transition or multiple memberships. The current study relies on the ability to describe image objects based on two types of membership, creating a meaningful land-cover classification of geographic features. These advantages are specific to an object-oriented approach.

2.4 Hierarchical data model

This study uses a hierarchical data model with an object-based approach to classifying detailed floodplain vegetation. The data structure was designed to mirror the relationships of real geographic features: individual woody plants (referred to as "Plant"), groups of woody plants (referred to as "Woody vegetation"), and functioning ecological units or habitats (referred to as "Segmented unit"). The previously identified geographic features are represented within the data model as non-overlapping polygons or objects at their appropriate map scales (Figure 3). Each horizontal level within the image object hierarchy shown in Figure 2 is made up of many instances of the image object below it; there is object overlap between different horizontal levels. For example, many plants make up a stand of woody vegetation. A woody vegetation stand shares a one-to-many cardinality with the individual woody plants within its extent. Not all woody plants within a stand of woody vegetation must be adjacent to each other. Similarly, the floodplains host many smaller habitats. This hierarchical model is conceptual and intended to illustrate the spatial relationships between features of differing sizes.

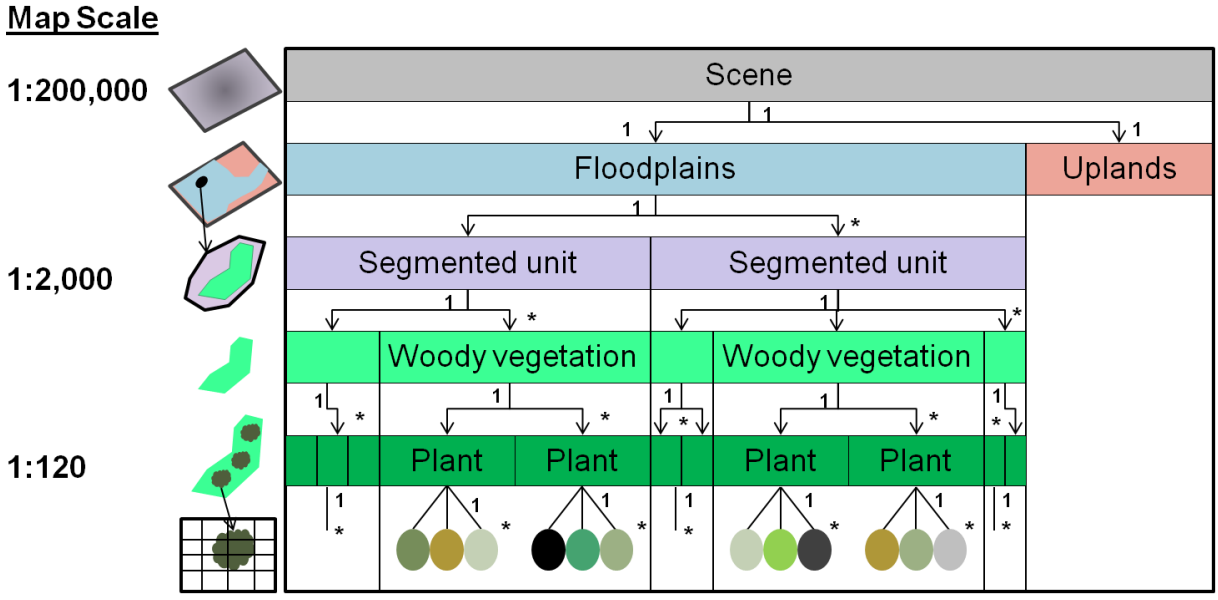

Figure 2: Data model and image object hierarchy for detailed vegetation classification. Each level represents a conceptual object type. Spatial resolution and map scale increases as object size decreases.

For the purposes of mapping detailed floodplain vegetation, we are interested in representing two types of geographic features as objects: individual habitats

(segmented units) and occurrences of natural woody vegetation. These two levels of objects were used as mapping units for this study. The spatial relationship of these two types of geographic features comprises the contextual information used to classify detailed vegetation land-cover classes. For the remainder of the paper, the term “segmented units” will refer to individual habitats while “woody vegetation” will refer to detectable occurrences of natural woody vegetation. Table 3 recaps key terms related to the hierarchical data model.

Segmented units are the minimum mappable units for the land-cover classes of interest. In other words, land-cover classification in this study occurs only at the segmented unit level. The segmented unit level is a geographic feature and image object that contains sub-objects (e.g., tree stands, shrub colonies, herbaceous patches) that determine its land cover. A segmented unit is spectrally distinct from neighboring objects at the desired mapping unit extent (in this case, 1:200 map scale or approximately 30 meters) that captures components of the ecological unit or habitat within its extent. For example, the finest resolution that a woodland (20-60% tree cover, DiGregorio 2005) can be observed should be the segmented unit, which includes both the open space and the trees. Within the eCognition image processing software, trial-and error tests as well as a comparison index (Weidner, 2008) between a non-systematic sample of habitats and image objects were used to determine the correct scale of these features. Segmented units are easy to conceptualize and observe in the field, but difficult to articulate into spectrally defined geographic features. Conceptually similar mapping units have been used by others for land cover mapping. Near the current study area, the Amazon Environmental Research Institute (IPAM) has been conducting a participatory mapping study which uses similarly defined mapping units for thematic classes of land use and cover (de Menezes 2014).

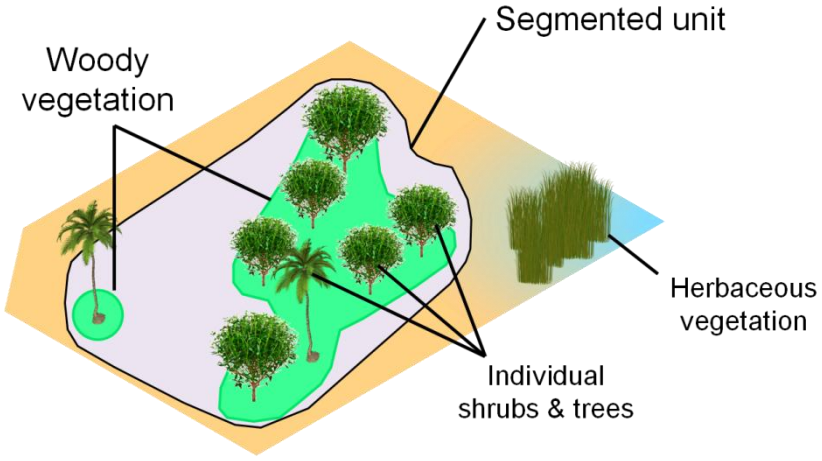

Figure 3: Example of relationships between geographic features (woody vegetation, segmented unit) used to define land-cover classes of interest. Woody vegetation is represented by the bright green polygons while the underlying segmented unit is the extent of the patch shown.

Figure 3 provides a conceptual example of a segmented unit. Two woody vegetation objects (bright green) are found within the supposed segmented unit (light

purple), which is characterized by bare soil (tan) outside of the woody vegetation objects. Because the nearby herbaceous vegetation is not part of the woodland shown and is part of a separate aquatic habitat, it is not part of the example segmented unit. Segmented units are found within but do not cover the entire floodplain, which is determined by an existing floodplain mask (Hess et al., 2003). Segmented units are mapped only where vegetation is present within the floodplain. Uplands are masked and subsequently excluded since they are not part of the land covers of interest (Figure 3).

The woody vegetation objects are occurrences of natural woody vegetation represented as sub-objects within individual habitats or segmented units. The woody vegetation objects capture the spatial extent of woody vegetation (including tree and shrub lifeforms at all detectable vertical levels and every density level) at very high resolution. The method used to identify woody vegetation is presented in section 4.4.1.

Term	Meaning	Associated data	Size
Pixel	Smallest unit of information in image; cell in array of data values	- Quickbird (QB) panchromatic & multispectral bands - Landsat 5 TM multispectral bands	0.6 m 2.4 m 30 m
Image object	Group of pixels grouped by 1+ criterion; relatively homogeneous and semantically significant; *meaningful objects for land-cover classification*	Image object primitives of segmented unit and woody vegetation objects	<25 m <5 m
Object	Vector data feature exported from an object-based image analysis software to GIS format	- Segmented unit - Woody vegetation	~30 m <30 m

Table 3: Key terms related to hierarchical data model and object-oriented land-cover classification

3. Data and study area

3.1 Study area

The study area covers a 17 kilometers by 39 kilometers longitudinal section of floodplains at the confluence of the Trombetas River and the Amazon River, immediately west of the town Oriximiná (Pará) as shown in Figure 4. The study area includes white water (várzea) and black or clear water (igapó) floodplains. The study area is part of the Lower Amazon region, which extends from the Amazonas and Pará state boundary east to the Xingu River confluence with the main Amazon River channel (Sheikh et al., 2006). A monomodal flood pulse inundates the floodplain for most of the year. Historical river stage data from Óbidos show that the river in this locality typically begins to rise in December, reaching its maximum height in June, and begins falling with increasing speed to reach its minimum level around early November (Melack and

Hess, 2010). The Lower Amazon floodplain consists of the main river channel and its ramifications, often forested marginal levees, a network of lakes that occupy the interior of the floodplain, and seasonally inundated grasslands occupying the transition zone between levee and permanent lakes. The region has a less complex topography and fewer distinct habitats than typically found upstream, and the limited forest cover consists mostly of secondary forests of varying ages (Wittmann et al., 2004). The dominant vegetation is characterized by grasslands composed of a variety of semi-aquatic macrophyte and shrub species (Costa, 2004).

In the Lower Amazon floodplain, human settlements and agricultural activities are concentrated on the levees, where lateral boundaries are often fenced and individual property rights are recognized and respected. This is in contrast to the grasslands inland from the local communities, which are usually treated as a commons and where cattle are allowed to circulate more or less freely within the zone (McGrath et al., 2007). Different plant communities and communities of different successional stages develop and result in a complex and highly diverse horizontal and vertical spatial structure of the floodplain habitats during the aquatic and terrestrial phases. Changes in water level, erosion, and sediment deposition modify the habitats and distributions of plant and animal communities.

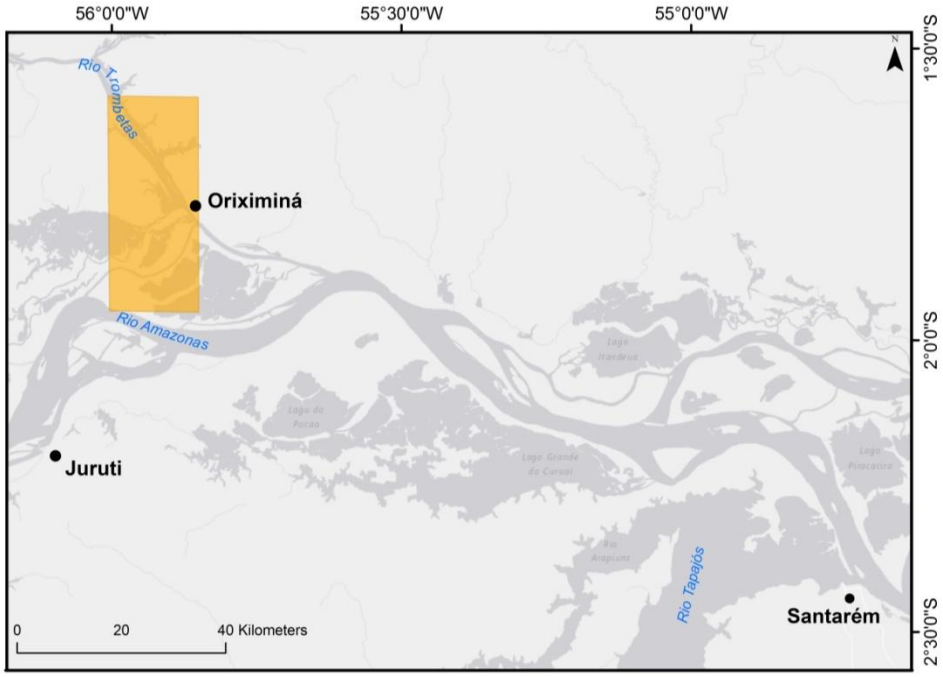

Figure 4: Study area overview in western half of Lower Amazon region, orange denotes study area. Base layer credit to ESRI World Light Gray Base map service (http://services.arcgisonline.com/ArcGIS/rest/services/Canvas/World_Light_Gray_Base/MapServer).

3.2 Data

Optical imagery was acquired at two different spatial resolutions-- three adjacent Quickbird 2 (29 October, 2005) scenes and one Landsat 5 Thematic Mapper (28 October, 2005; path 228, row 61) scene (Figure 2). Both datasets feature minimal cloud cover and are cotemporaneous at the lowest water stage of the 2005 drought. Minimizing the occurrence of cloud cover and extent of inundation is necessary to identify and classify non-forest vegetation as seasonal water level variability is enough to cover much of the shrubs and herbaceous vegetation.

3.2.1 Information required for detailed vegetation classification

For multispectral imagery, spectral information based on a single pixel of any resolution alone generally does not provide enough information to yield a detailed vegetated land-cover classification. The spectral differences between the vegetated land-cover classes of interest in this study are quite subtle, making separability of vegetation structures and lifeforms difficult. To address this challenge, a variety of different spatial and spectral resolution image bands were used to generate higher level data as input for determining an overall land-cover classification.

Very high resolution panchromatic imagery: The panchromatic band of the Quickbird imagery, a 0.6 meter spatial resolution with a spectral range of 405-1053 nanometers, was used to derive image texture index. Surface reflectance values of this very high spatial resolution band are extremely variable, but adequately capture the heterogeneous pattern of woody vegetation structures against underlying materials.

High resolution panchromatic imagery: The multispectral bands (blue, green, red, near infrared) of the Quickbird imagery, a 2.4 meter spatial resolution with single band spectral ranges averaging 148 nanometers for the four bands, provide spectral information at fine scales, useful in separating vegetation from non-vegetation.

Medium resolution multispectral imagery: The multispectral bands (blue, green, red, near infrared, and short wave infrared) of Landsat 5 TM imagery, a 30 meter spatial resolution for non-thermal bands with single band spectral ranges averaging 124 nanometers for the five bands, were used as input for spectral mixture analysis.

3.2.1 Image pre-processing

The Landsat 5 TM and Quickbird 2 datasets were pre-processed based on the respective information needs of the object-based classification. The Landsat 5 TM scene entirely covers the study area. Surface reflectance, a high-level product available as part of the Landsat Climate Data Record, in bands 1-5 and 7 were clipped to the study area. Surface reflectance data are generated from a MODIS-based atmospheric

correction and other inputs using the Landsat Ecosystem Disturbance Adaptive Processing System (USGS 2015). Three vertically adjacent Quickbird scenes, which cover an area 17 kilometers wide by 39 kilometers long, were mosaicked without additional corrections since the geometric and radiometric differences between the scenes were not significant. The multispectral bands were resampled to 0.6 m pixel size using a nearest neighbor algorithm to match the panchromatic band.

A floodplain mask was applied to the Quickbird mosaic by clipping the data to the extent of the Amazon wetlands mask produced by Hess et al. (2003). The Amazon wetlands mask covers the Amazon River main stem and major confluences, but did not include approximately 6 kilometers of clear water floodplains along the Trombetas River. The extent of the floodplains not covered by the Amazon wetland mask was digitized and appended to the existing Amazon wetland mask. To reduce processing time, the Quickbird mosaic was subset into three separate image regions using canals as breaks between distinct landforms. Each of the three image regions was processed separately using the same workflow, then merged with the other regions in polygon layers covering the extent of the study area. Additionally, urban areas and rural settlements were excluded because they are not part of the vegetation classes of interest; only subclasses of natural or semi-natural land covers are addressed in this study.

4. Methods

4.1 Image segmentation

Object-based image analysis (OBIA) is a growing sub-discipline of Geographic Information Science that seeks to develop automated methods to partition remote sensing imagery into meaningful geographically based image objects and assess their characteristics through spatial, spectral, and temporal scales. OBIA requires image segmentation, attribution, and classification resulting in the ability to query and link individual objects (Blaschke et al., 2014).

Image segmentation is a principal function that splits an image into separated regions or objects depending on the parameters specified (Myint et al., 2011). A group of pixels having similar spectral and spatial properties is considered an object. For this study, all image segmentations and the delineation of woody vegetation objects was completed with the Trimble eCognition software (Definiens, 2008). Within eCognition, the multiresolution segmentation algorithm was used to generate medium-scale image objects for segmented units and fine-scale image objects for woody vegetation classification. It is a bottom-up region growing technique that groups pixels according to an optimization function that minimizes intra-object spectral and spatial heterogeneity (Equation 1, Definiens 2008):

$$w_{spectral} * h_{spectral} + \left(1 - w_{spectral}\right) * h_{spatial} \leq h_{scale} \qquad \text{(Equation 1)}$$

where $h_{spectral}$ measures the spectral variability within the object; $h_{spatial}$ characterizes the object shape, and $w_{spectral}$ inversely weights $h_{spectral}$ and $h_{spatial}$. The merging procedure continues until the within-object heterogeneity exceeds the user-defined threshold h_{scale} (Baatz and Schäpe, 2000). Parameters used for the two image segmentations are listed in Table 4. The parameters chosen are based on iterative testing and nearest match of a comparison index (Weidner, 2008).

Object type	h_{scale} Scale	$h_{spatial}$ Shape	$h_{spectral}$ Compactness	Bands used
Segmented unit	300	0.3	0.1	Quickbird multispectral, 2:1 weight near infrared to visible
Woody vegetation	6	0.6	0.3	Quickbird panchromatic band

Table 4: Multiresolution segmentation parameters for object types of interest

4.2 Sub-pixel analysis

Sub-pixel analyses seek to determine the percentage of cover of a given material or land cover within a pixel. In this study, a sub-pixel analysis (spectral mixture analysis) was conducted to provide additional spectral information to be aggregated within woody vegetation image object. These data were intended to delineate different woody lifeforms, like trees and shrubs, assuming that compositional differences between these lifeforms are sufficiently different to be spectrally detectable at the available spatial, spectral, and radiometric resolutions.

4.2.1 Spectral mixture analysis

Spectral mixture analysis (SMA) is a commonly used method of quantifying the relative abundance of surface materials within a pixel. Spectral mixture analysis models pixel spectra as a linear combination of the spectral signatures of two or more material components (Equation 2), referred to as endmembers, as fractions of the pixel that material covers. An endmember is the spectrum of a pure material component (e.g., green vegetation, non-photosynthetic vegetation, soil). SMA is based on the assumption that the reflectance (*P'*) measured at pixel *i* can be modeled as the linear sum of *N* endmembers weighted by the fraction f_{ki} of each endmember within the field of view of pixel *i* (Adams et al. 1993). For a given wavelength (λ):

$$P'_{i\lambda} = \sum_{k=1}^{N} f_{ki} * P_{k\lambda} + e_{i\lambda} \qquad \text{(Equation 2)}$$

where $e_{i\lambda}$ is a residual term indicating the disagreement between the measured and modeled spectra. The modeled fractions are constrained to equal 1.

There is a significant challenge in identifying and capturing spectra for pure components, particularly in dynamic environments like the Lower Amazon floodplain. Previous work in the study area by Powell et al. (2013) used Multiple Endmember Spectral Mixture Analysis (Roberts et al., 1998) to iteratively test and build a spectral

library using Landsat 5 TM FLAASH-corrected imagery. The spectral library created by Powell et al. (2013) was used in this study. A three endmember (green vegetation, non-photosynthetic vegetation, and shade) model with endmember fraction constraints (-0.05 to +1.05) was applied to the Landsat 5 TM image. With these constraints, 97% of the pixels within the floodplains were modeled.

Upon generation of endmember fractions for green vegetation, non-photosynthetic vegetation, and shade of the Landsat image, endmember fraction floating value rasters were resampled to 0.6 meter cells and clipped to the extent of the woody vegetation objects (by geometric intersection). All endmember fraction values within an individual woody vegetation object were averaged and recorded to that object ($n = 9{,}038$ objects). Figure 5 shows the distribution of the average endmember fractions at the woody vegetation object level. If our assumption holds true that compositional differences between tree- and shrub-dominanted areas are detectable by significant differences in endmember fraction values, then we would expect to see bimodal distributions of endmember fractions.

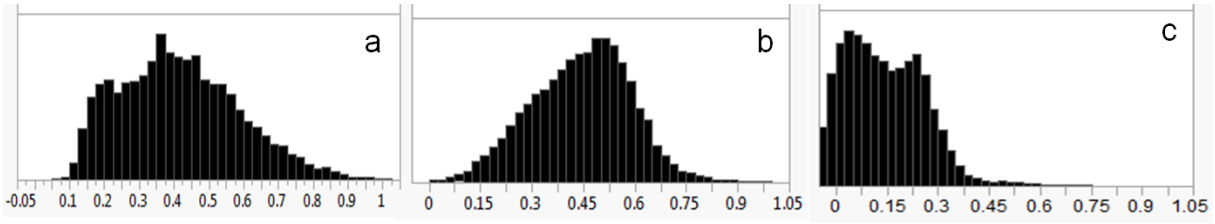

Figure 5: Average green vegetation (a), non-photosynthetic vegetation (b), and shade (c) endmember fractions within woody vegetation image objects

4.3 Classification methods

Previous steps were used to generate information for the purpose of detailed vegetated land-cover classification. In creating the final land-cover classification map, three additional vegetation maps were produced, each of which is a contribution to high resolution vegetation mapping. The three additional vegetation maps include extent of woody vegetation at <30-meter resolution (section 4.3.1), a calculation of wood vegetation cover within individual habitats/segmented units (section 4.3.2), and the dominance of tree or shrub physiognomies within individual habitats/segmented units (section 4.3.3). Figure 6 provides a workflow that details steps in detailed vegetated land-cover classification.

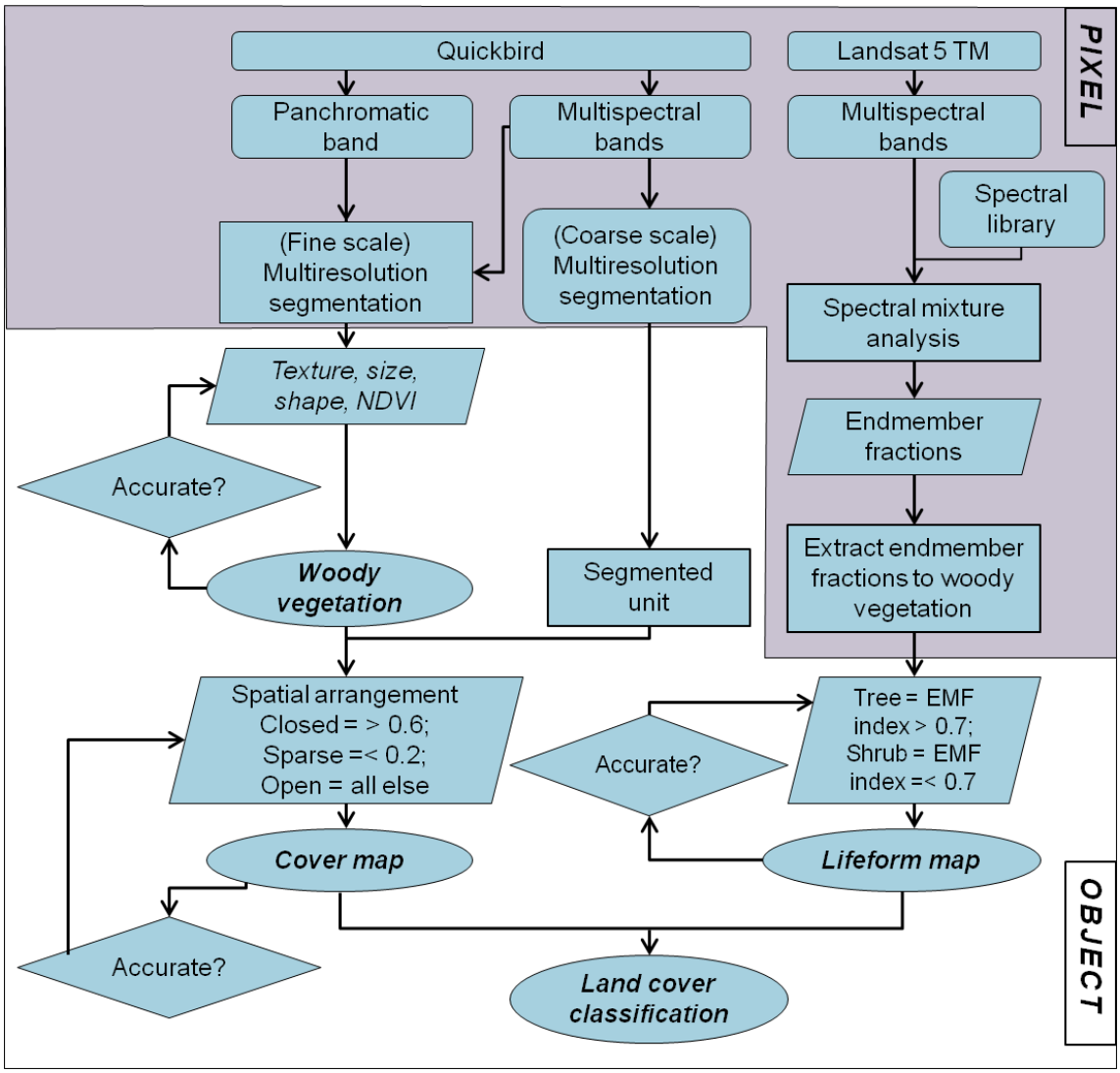

Figure 6: Workflow for hierarchical object-based classification of detailed floodplain vegetation classification

4.3.1 Woody vegetation delineation

Delineating woody vegetation at <30-meter resolution accomplishes two goals: calculation of total area covered by detectable levels of woody vegetation and spatial distribution, and elimination of areas without woody vegetation (with similar or confusing endmember fraction values) from the classification process. The delineation of woody vegetation in this study relies on the heterogeneity vegetation shows as a result of irregular shadow or shade (Ehlers et al., 2003) which makes it distinguishable from the surrounding materials. A combination of image texture derived from the Quickbird panchromatic band and spectral properties from the Quickbird multispectral bands were used to delineate woody vegetation.

Image texture indices have high potential to measure and monitor vegetation structures at landscape scales (Blaschke, 2003). An adaptive filter was used to process the computationally intensive very high resolution panchromatic band data. Adaptive filters are based on the assumption that the mean and variance of the pixel of interest are equal to the local mean and variance of all pixels within the user-selected moving window or neighborhood. The Lee-sigma filter uses sigma probability of the Gaussian distribution to average pixels within a given neighborhood that have intensities (brightness) within a fixed sigma range of the center pixel (Lee, 1983). For this application, a 2-sigma probability (p=.955) was used with a neighborhood of 9x9 pixels for dark and light edge extractions. The filter window neighborhood (5.4 x 5.4 meters) reflects the average size of the woody vegetation objects to be mapped. With the Lee-sigma filter, subtle details are retained and ramp edges are sharpened, which typically characterize gradual transitions between types of natural vegetation in the aquatic-terrestrial transition zone. A roughness index was created by normalizing the sum of the light and dark edge extraction layers by the brightness for each pixel. The customized roughness index enhances the textural differences between woody and non-woody vegetation as well as non-vegetated surfaces (turbid water, sand).

A rule-based classification was created in eCognition to delineate woody vegetation using the high-resolution multiresolution segmentation image objects based on four object statistics (roughness index, normalized difference vegetation index, object length-to-width ratio, and near infrared reflectance). Object shapes were refined in cases of oversegmentation and edge artifacts by using area and area relative to neighbor attributes to merge objects. The result, shown in Figure 7, is a very high resolution (<30-meter) vector layer that represents the extent of woody vegetation.

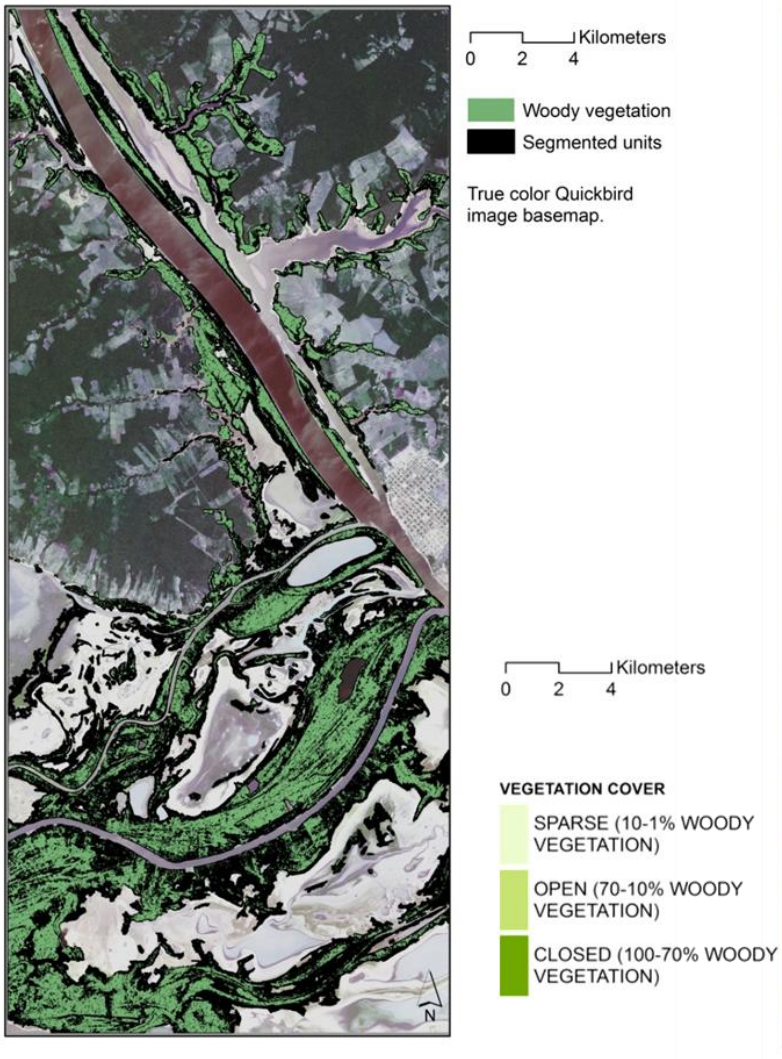

Figure 7: Results of woody vegetation classification

Figure 8: Results of vegetation cover classification

4.3.2 Vegetation cover classification

Vegetation cover defines the spatial arrangement of vegetation lifeforms and can be considered as the presence of a particular area of the ground, substrate, or water surface covered by a layer of plants considered at the greatest horizontal perimeter level of each plant in the layer (Eiten, 1968). Cover can be specified as the horizontal extent of vegetation within a map unit as well vegetation height. Cover was quantified by calculating the proportion of a segmented unit that is geometrically intersected or covered by the woody vegetation objects. This proportion is expressed as a percent of segment unit covered, fitting into predefined classes used by the Land-cover classification System (Table 1). These predefined classes include Closed (>70%), Open (20-70%), and Sparse (<20%). The result of this classification, shown in Figure 8, is a high resolution (30-meter) vector layer that specifies the proportion of an area covered by woody vegetation.

4.3.3 Woody vegetation lifeform classification

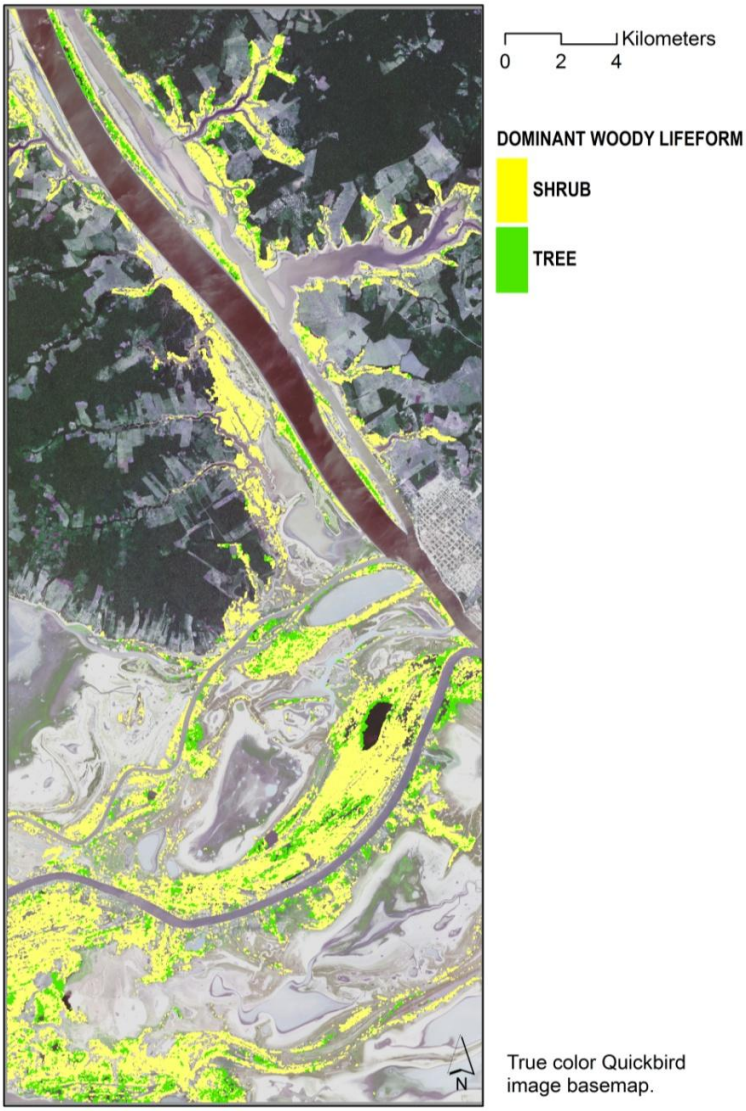

Figure 9: Results of dominant woody vegetation lifeform classification

Lifeform of a plant is defined by its physiognomic aspect, specified in this case as shrub or tree. This classification is independent of vegetation cover and dependent on the estimated quantity of ground materials from a sub-pixel analysis. As discussed in section 4.3, endmember fractions generated using spectral mixture analysis were aggregated at the woody vegetation object level for vegetation lifeform classification. Endmember fraction averages from the woody vegetation objects were then averaged to the coinciding segmented unit. Each woody vegetation object was weighted equally regardless of size. Several classification techniques were tested, including supervised and unsupervised nearest neighbor classifications within eCognition, a maximum likelihood classification based on known proportion distribution of lifeforms in this part of the floodplain (Sheikh et al., 2006; Reno et al., 2011), Getis-Ord General G high/low cluster classification, and a weighted endmember fraction index threshold.

The Getis-Ord General G cluster classification correctly classified segmented units with very low lifeform variability. Ultimately, the weighted index threshold was used because it most consistently classified mixed and single lifeform-dominant woody vegetation objects within segmented units. Based on previous work (Souza Jr. et al., 2003) where shade fraction was a stronger predictor of intact tree stands, a simple linear weighted index was created to distinguish tree and shrub lifeforms. The index (Equation 3) ranged from 0 to 2 with values near 2 classified as tree and values less than 1 classified as shrub.

$$Lifeform = 0.3 * f_{Green\ vegetation} + 0.7 * f_{Shade} \quad \text{(Equation 3)}$$

A one-way between classes ANOVA was conducted to compare the average endmember fractions between segmented units classified as shrub and as tree, which found that there was a significant difference in average shade fraction between classified lifeforms at the 95% confidence level (F(1, 9,037)=4.28, p=0.03) but not a significant difference in average green vegetation fraction between classified lifeforms at the 95% confidence level (F(1, 9,037)=2.53, p=0.11). The result of this classification, shown in Figure 9, is a high resolution (30-meter) vector layer that maps habitats dominated by shrub or tree lifeforms.

4.3.4 Detailed vegetated land-cover classification

An object-based classification was created and automated for use in a Geographic Information System using the preceding vegetation maps to classify vegetated land cover in the floodplains. The object-based classification scheme uses Boolean logic to combine the land-cover class attributes for cover and lifeform within comprehensible class names defined by the Land-cover classification System. The result of this classification, shown in Figure 10, is a high resolution (30-meter) vector layer that shows the results of the detailed land-cover classification for (semi-)natural regularly flooded vegetation.

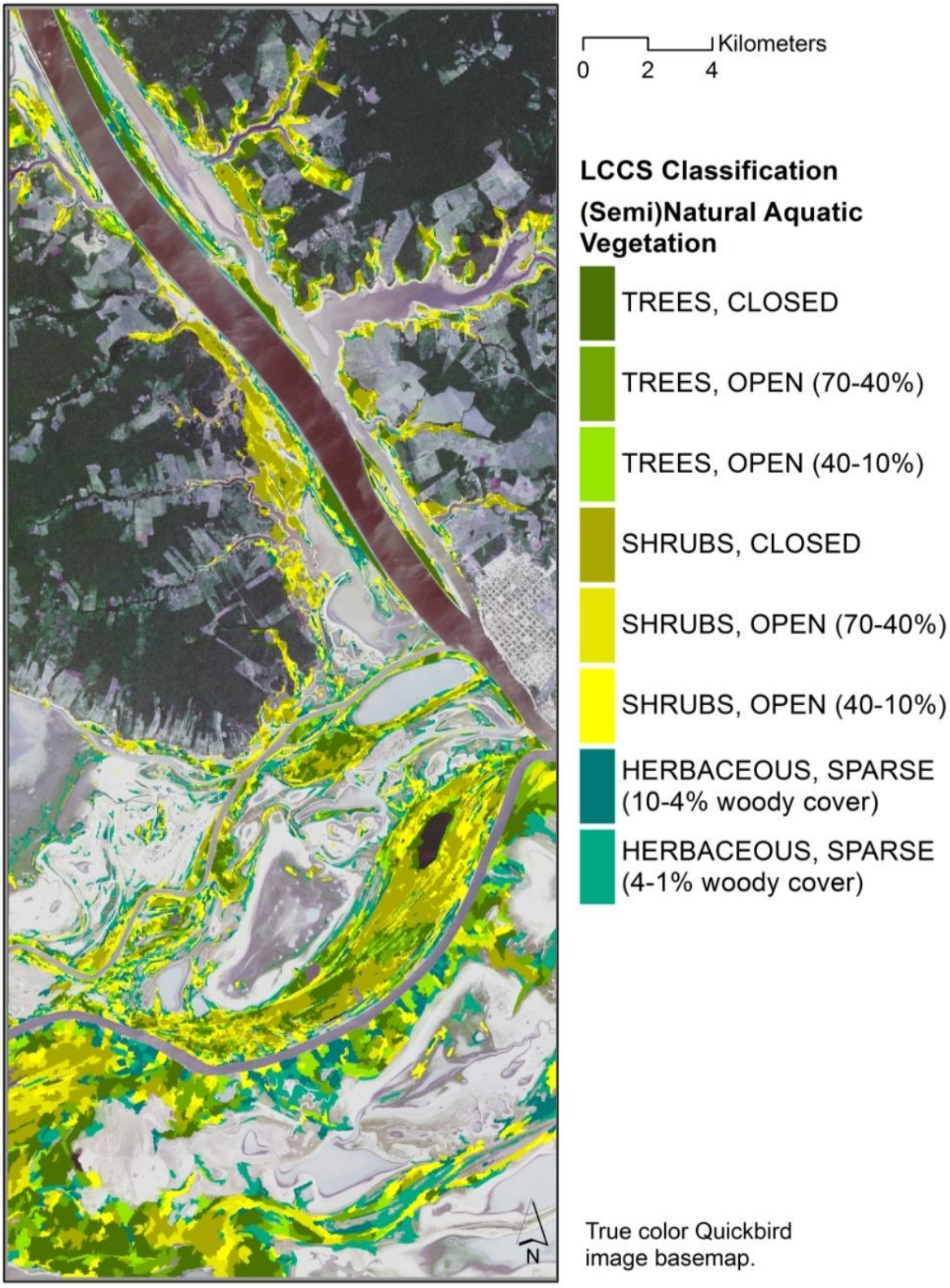

Figure 10: Detailed vegetated land-cover classification results

5. Accuracy assessment

Assumptions and errors accumulate from the base woody vegetation delineation to the detailed vegetated land-cover classification. Since this study focuses on vegetation across multiple spatial scales, accounting for accuracy at each stage of the overall classification is warranted. Unless otherwise specified, the accuracy of each classification was assessed using 160 validation objects randomly distributed and spatially balanced within the study area. The validation points were manually interpreted and coded for the required Land-cover classification System classifiers, Lifeform and Cover, using the same Quickbird scenes. The manual image interpretations were compared to the classification maps to build error matrices and derive overall accuracy, class accuracy, kappa statistics (Congalton 1991). In error matrices, the diagonal cells with the same category at each axis indicate correctly mapped samples. All other observations indicate a misclassified reference sample. Overall accuracy refers to the number of correctly classified samples divided by the total number of samples. Producer's accuracy measures within each column of the matrix to identify errors of omission, which occurs when a reference sample is misclassified. Producer's accuracy is useful to gauge the likelihood of an object being classified correctly given it is a certain class, thus is useful for describing classification accuracy. User's accuracy measures within each row of the matrix to identify errors of commission, which occurs when a class is assigned to a sample but it is not actually present. User's accuracy is useful to gauge the likelihood of correctness of an object's classification, thus is useful for describing class accuracy. Kappa (Cohen 1960) is a measure of overall accuracy that takes agreement by chance into account. In these statistics, all errors are equally weighted.

5.1 Woody vegetation classification accuracy assessment

Reference data was created by creation of a 5,000 point digitized sample of crown centroids from individual woody plants (4,000 points) and areas without woody plants (1,000 points). The sample centroids without woody vegetation were selectively digitized at the edges of woody vegetation clusters or stands. Because the reference data lack field verification and the available image resolution, the reference data are sufficient only to evaluate spatial extent of woody vegetation. Table 5 shows the confusion matrix of the classification. The overall accuracy of this classification is moderately high (86%) with elevated levels of woody vegetation omission (85%) and not woody vegetation commission (38%). Of the tree centroids that were omitted by the woody vegetation classification, 80% of the omitted tree centroids were location within 30 meters of classified woody vegetation. Of the woody vegetation image objects that were sources of commission error, many were observed to extend just over the interpreted edge of the actual woody vegetation. The separation between classified woody vegetation and non-woody vegetation areas is not as definitive based on the image object boundaries, but is more general and true proportion at the scale of the segmented unit.

	REFERENCE			
CLASSIFIED	Woody vegetation	Not woody vegetation	Total	User's accuracy
Woody vegetation	3910	11	3921	0.99
Not woody vegetation	676	403	1079	0.38
Total	4586	414	5,000	
Producer's accuracy	0.85	0.97		**κ=0.48** **$SE_κ$=0.016**

Table 5: Error matrix for woody vegetation classification

5.2 Vegetation cover accuracy assessment

The cover classification is the most robust and accurate classification generated in this study. It is based on the spatial relationship of woody vegetation classified objects to their surroundings, which is less prone to significant differences in result unless segmented units are dramatically altered in scale and size. Table 6 shows the confusion matrix of the classification. It has the highest overall accuracy (94%) with the most consistency between classes of all classifications used. The highest errors were observed for sparse cover, with an omission error of 14% from evenly split misclassification between open and closed cover. The remaining classes had omission errors of 2% (open cover and closed cover). Conversely, open and closed covers had the lowest commission errors (6%) while sparse cover had a slightly higher rate of commission errors (5%). Since the objective of this research was to identify open and closed covers and the classification for sparse cover is based solely on woody vegetation abundance (according to sub-condition of cover rule), higher omission error rates are acceptable for sparse cover.

		REFERENCE				
		Sparse	Open	Closed		User's
CLASSIFIED		A24A16	A24A13	A24A12	Total	accuracy
Sparse	A24A16	42	1	1	44	0.95
Open	A24A13	4	59	0	63	0.94
Closed	A24A12	3	0	50	53	0.94
	Total	49	60	51	160	
Producer's accuracy		0.86	0.98	0.98		**κ=0.92** **$SE_κ$=0.04**

Table 6: Error matrix for vegetation cover classifier

5.3 Vegetation lifeform accuracy assessment

The vegetation lifeform classifier performed well with an overall accuracy of 90%. The highest rate of omission errors was observed for tree lifeform (12%) while both shrub and herbaceous lifeforms had lower omission error rates (9% and 6%

respectively). Table 7 shows the confusion matrix of the classification. This pattern was repeated by commission errors, indicating a general confusion regarding the tree lifeform class. Whereas trees are generally the easiest vegetation forms to classify, the physiognomic distinctions between tree and shrub are very subtle. The confusion of trees as shrubs is likely a result of assuming shrub life forms as default lifeform since they dominate the floodplains of the Lower Amazon region.

		REFERENCE				
		Shrub	*Tree*	*Herbaceous*		User's
CLASSIFIED		A24A4	A24A3	A24A2	*Total*	accuracy
Shrub	A24A4	77	4	1	*82*	0.94
Tree	A24A3	5	36	1	*42*	0.86
Herbaceous	A24A2	3	1	32	*36*	0.89
	Total	*85*	*41*	*34*	*160*	
						κ=0.85
	Producer's accuracy	0.91	0.88	0.94		**$SE_κ$=0.04**

Table 7: Error matrix for dominant vegetation lifeform classification

5.4 Land cover accuracy assessment

Validation of the detailed floodplain vegetation classification based on comparison with 255 manually interpreted sample objects using the same Quickbird imagery yielded an overall accuracy of 75% and kappa index of 0.68 (Table 8). Combining the error of the preceding classifications, the detailed vegetated land-cover classification is moderately accurate overall. Certain classes (closed and open tre) are overestimated while other classes (open tree and herbaceous) are underestimated. Most of the confusion between classes came from misclassification between lifeforms of the same cover level (e.g., shrub as tree, tree as shrub).

The resulting detailed floodplain vegetation classification reveals a dominance of closed shrubs and general herbaceous cover with an overall complex distribution of vegetation structure and dominant life forms. Woody vegetation was distributed as 18% (29,879 m^2) of forest, 13% (23,448 m^2) of woodland, 20% (34,616 m^2) of closed shrub, 26% (46,291 m^2) of open shrub, and 23% (40,490 m^2) of herbaceous cover. This distribution of land cover types is different than previously reported (Reno et al., 2011; Sheikh et al., 2006). However, the classifications used in this study differ substantially in class definitions for overall land-cover classes. These results are explicit about the land-cover class definitions and criteria, as opposed to generalized descriptions of non-forest vegetation or land uses. Additionally, these results are highly location specific and can be referenced throughout time to monitor changes in cover or dominant lifeform.

	REFERENCE						
CLASSIFIED	Tree, Closed	Tree, Open	Shrub, Closed	Shrub, Open	Herbaceous, Sparse Woody Vegetation	*Total*	User's accuracy
Tree, Closed	38	5	3	0	1	*47*	.81
Tree, Open	1	31	0	5	2	*39*	.79
Shrub, Closed	11	0	40	4	6	*61*	.66
Shrub, Open	1	10	2	33	12	*58*	.57
Herbaceous, Sparse Woody Vegetation	1	0	0	1	48	*50*	.96
Total	*52*	*46*	*45*	*43*	*69*	*255*	**κ=0.68** **SE_κ=0.03**
Producer's accuracy	.73	.68	.89	.77	.70		

Table 8: Error matrix for detailed vegetated land-cover classes (LCCS scheme)

6. Discussion

Because the detailed floodplain vegetation land cover map was synthesized using multiple data products, there are multiple potential sources of error. At every point in the creation of the modular classifier maps, uneven responses at every spatial extent add confusion to higher level results. The most significant source of potential error is in the delineation of woody vegetation. The overall accuracy of this classification is high (86%), but this base level of error is inherited throughout the remaining classifications. The propensity for errors of commission in the woody vegetation classification resulted in a possible overestimation of woody cover and underestimation of herbaceous cover not defined by an absence of woody vegetation. However, the utility of spatial relationships between objects of different scales is clear given the accuracy and strength of agreement of the vegetation cover classification.

No finer scale classification (e.g., tree crown or individual plant) is necessary to achieve the objectives of this study. Sub-objects of woody vegetation, such as individual plants and individual plant structural features, and their relationships to the coarser woody vegetation classification are meaningful. However, the spatial scale of high resolution imagery does not provide enough information to delineate individual plants. The minimum pixel to object ratio for tree crown delineation is 9:1 with the optimal ratio at 15:1 (Larsen et al., 2011). The pixel to object ratio for the averaged size tree crown (3.2 meters diameter) in the study area is 4:1, much lower than the minimum recommended pixel to object ratio.

The next highest source of error comes from the sub-pixel analysis, which includes residuals from linear regressions. The effect of aggregating pixel endmember

fractions at an appropriate image object level is that endmember fractions become more robust to intra-object variability, which is a known limitation of using sub-pixel approaches in land-cover classification. Conversely, aggregation of pixel-based values in a bottom-to-top manner is an easily skewed process. The order of allocating endmember fraction values at different spatial scales merits consideration to avoid over-generalizing fractions.

Using multiple data sources and data products at multiple spatial scales is an effective strategy to distinguish subtle features and land-cover classes. In this case, a hierarchical object-oriented approach can mirror the relationship of the represented geographic features with discrete objects. The components of these land-cover classes exist as elements inextricably linked by place. Mapping components as continuous fields preserves data values but loses understandable description. The methods used in this study can be applied to other regularly flooded or other environment characterized by heterogeneity with sufficient adaptation of the current methods. Additional work should be done to fully automate this workflow between platforms and to address subjectivity in design.

The exact ranges and definitions of classification criteria used in this study may not be best suited for the Lower Amazon floodplain. Herbaceous vegetation plays a much more important role in understanding spectral response throughout the scene than given attention here, particularly where mixed vegetation lifeforms are present. For a more complete picture of the floodplain vegetation distribution, hydrological, geomorphological, and botanical characteristics ought to be included to create a comprehensive classification (Junk et al., 2012). Floodplain vegetation can be consistently and accurately mapped without additional hydrological information. Based on the applicability of these findings to Amazonian wetland studies and land-cover classification literature, we encourage the use of systematic land-cover class definitions in the future. The ability to relate current and past studies to each other is critical to developing a robust understanding of changing floodplain vegetation, increased land pressures, and varying flood regimes.

7. Conclusion

Using low-water stage very high resolution and moderate resolution multispectral optical imagery, this project has mapped detailed floodplain vegetation at 30-meter resolution for a 663 square kilometer area of the Lower Amazon region. Detailed floodplain vegetation is distinguished by cover (horizontal vegetation extent) as well as dominant vegetation lifeform (physiognomy) for this application, as prescribed by the Land-cover classification System. Woody vegetation extent was delineated using a rule-based classification (overall accuracy of 86%) of very small image objects by a combination of texture, spectral, and shape values. Within the woody vegetation portion of the study area, data products from a sub-pixel (spectral mixture) analysis were extracted and averaged among those small woody vegetation objects. These woody vegetation image objects were compared to coarser image objects representing

landscape patches or individual habitats. The coarser landscape patch objects are classified by woody vegetation cover within their extents (94% overall accuracy) and dominant vegetation lifeform (90% overall accuracy) as inferred from differences in endmember fractions. The resulting detailed floodplain vegetation classification (75% overall accuracy) reveals a dominance of closed shrubs and general herbaceous cover with an overall complex distribution of vegetation structure and dominant life forms. Woody vegetation was distributed as 18% (29,879 m^2) of forest, 13% (23,448 m^2) of woodland, 20% (34,616 m^2) of closed shrub, 26% (46,291 m^2) of open shrub, and 23% (40,490 m^2) of herbaceous cover. The results show that by using a combination of pixel and object-based approaches, multispectral imagery can be used to quantify areal vegetation cover and vegetation type. The mapping method presented has general applicability to mapping woody vegetation in wetlands and heterogeneous areas characterized by quantity or type of woody vegetation.

ACKNOWLEDGEMENTS

I would like to acknowledge my advisor, Dr. Rebecca L. Powell (University of Denver), for her insight and advice throughout this project as well as my reader, Dr. Jing Li (University of Denver) for her assistance throughout this research. Additionally, Dr. Laura L. Hess (University of California- Santa Barbara) has been critical for the opportunity and data to conduct this research. This research was undertaken and supported as part of the “Land and Resource Use on the Amazon Floodplain Under Evolving Management Systems and Environmental Change: Fish, Forests, Cattle, and Settlements” project through the NASA Land-Cover/Land-Use Change Program. Quickbird satellite imagery was provided through NASA partnership and Landsat TM CDR imagery was acquired via Earth Explorer data portal from the United States Geological Survey.

REFERENCES

Addink, E.A., de Jong, S.M., Pebesma, E.J., 2007. The importance of scale in object-based mapping of vegetation parameters with hyperspectral imagery. *Photogrammetric Engineering & Remote Sensing* 73 (8): 905-912.

Adams, J. and A. Gillespie. 2006. *Remote Sensing of Landscapes with Spectral Images: A Physical Modeling Approach*. Cambridge University Press: London.

Adams, John B., Donald E. Sabol, Valerie Kapos, Raimundo Almeida Filho, Dar A. Roberts, Milton Smith, and Alan R. Gillespie. 1995. Classification of Multispectral Images Based on Fractions of Endmembers: Application to Land-Cover Change in the Brazilian Amazon. *Remote Sensing of the Environment* 52:137-154.

Asner, G. P. and K. B. Heidebrecht. 2002. Spectral unmixing of vegetation, soil and dry carbon cover in arid regions: comparing multispectral and hyperspectral observations. *International Journal of Remote Sensing* 23(19), 3939-3958.

Baatz, M., & Schäpe, A. (2000). Multiresolution segmentation —An optimization approach for high quality multi-scale image segmentation. XII Angewandte Geographische informationsverarbeitung (pp. 12–23). Salsburg.

Barbosa, C., L. Hess, J. Melack , E. Novo , M, Gastil , and L. Dutra. 2000. Mapping Amazon Basin Wetlands through Region Growing Segmentation and Unsupervised Region Classification of JERS-1 Data. *INPE*, accessed 10/15/13 http://www.dpi.inpe.br/geopro/trabalhos/artigo_japao.pdf.

Benz, U.C., P. Hofmann, G. Willhauck, L. Lingenfelder, and M. Heynen. 2004. Multi-resolution, object-oriented fuzzy analysis of remote sensing data for GIS-ready information. *ISPRS Journal of Photogrammetry and Remote Sensing* 58(3-4): 239-258.

Blaschke, T. 2010. Objet based image analysis for remote sensing. *ISPRS Journal of Photogrammetry and Remote Sensing* 65:2-16.

Blaschke, T., Hay, G. J., Kelly, M., Lang, S., Hofmann, P., Addink, E., Feitosa, R. Q., van der Meer, F., van der Werff, H., van Coillie, F., & Tiede, D. 2014. Geographic object-based image analysis–towards a new paradigm. *ISPRS Journal of Photogrammetry and Remote Sensing* 87:180-191.

Brondizio E, E. Moran, P. Mausel, and Y. Wu. 1996 Land cover in the Amazon estuary – linking of the thematic mapper with botanical and historical data. *Photogrammetric Engineering and Remote Sensing* 62:921–929.

Burnett, C., Blaschke, T., 2003. A multi-scale segmentation/object relationship modelling methodology for landscape analysis. *Ecological Modelling* 168 (3), 233-249.

Castello, L., D. G. McGrath, L. L. Hess, M. T. Coe, P. A. Lefebvre, P. Petry, M. N. Macedo, V. F. Réno, and C. C. Arantes. 2013. The vulnerability of Amazon freshwater ecosystems. Conservation Letters 0:1-13.

Congalton, R. 1991. A review of assessing the accuracy of classifications of remotely sensed data. Remote Sensing of Environment 37:35-46.

Costa, M. P. F. 2004. Use of SAR satellites for mapping zonation of vegetation communities in the Amazon floodplain. *International Journal of Remote Sensing* 25(10), 1817-1835.

Definiens. 2008. Definiens developer 8: User guide. The Imaging Intelligence Company, Munich.

DiGregorio, A. 2005. Land-cover classification System: Classification concepts and user manual. Food and Agriculture Organization of the United Nations: Rome.

Ehlers, M., M. Gahler, R. Janowsky. Automated analysis of ultra high resolution remote sensing data for biotope type mapping: new possibilities and challenges. *ISPRS Journal of Photogrammetry and Remote Sensing* 57(5), 315-326.

Eiten, G. 1968. Vegetation Forms. A classification of stands of vegetation based on structure, growth form of the components, and vegetative periodicity.*Boletim do Instituto de Botanica, San Paulo,* (4): pp. 67.

Fernandez-Manso, O., A.F. Manso, and C. Q. Pastor. 2005. Combining spectral mixture analysis and object-based classification. *Investigation agraria*, 18(3): 296-313.

Ferreira-Ferreira, J., T. S. F. Silva, A. S. Shreher, A. G. Affonso, L. F. de Almeida Furtado, B. R. Forsberg, J. Valsecchi, H. L. Queiroz, and E. M. L. de Moraes Novo. 2015. Combining ALOS/PALSAR derived vegetation structure and inundation patterns to characterize major vegetation types in the Mamirauá Sustainable Development Reserve, Central Amazon Floodplain, Brazil. *Wetlands Ecological Management* 23(2015):41-59.

Ford-Robertson, F.C. 1971. *Terminology of Forest Science, Technology Practice and Products.* Society of American Foresters, Washington DC.

Hall, O., Hay, G.J., Bouchard, A., Marceau, D.J., 2004. Detecting dominant landscape objects through multiple scales: An integration of object-specific methods and watershed segmentation. *Landscape Ecology* 19 (1), 59-76.

Hay, G.J. and G. Castilla. 2008. Geographic Object-Based Image Analysis (GEOBIA): a new name for a new discipline. In: Blaschke, T., Land, S., Hay, G. (eds), *Object-Based Image Analysis*. Springer, New York, pp. 75-89.

Hess, L. L, J. M. Melack, E. M. L. M. Novo, C. C. F. Barbosa, and M. Gastil. 2003. Dual-season mapping of wetland inundation and vegetation for the central Amazon basin. *Remote Sensing of the Environment* 87:404-428.

IPCC. 2007. Intergovernmental Panel on Climate Change AR4 Synthesis report, IPCC Secretariat, Geneva, Switzerland.

Junk, W. 1997. The Central Amazon Floodplain: Ecology of a Pulsing System, *Ecological Studies* 126. Springer.

Junk, W. J., M. T. F. Piedade, J. Schöngart, and F. Wittmann. 2012. A classification of major natural habitats of Amazonian white-water river floodplains (várzeas). Wetlands Ecology and Management 20(6):461-475.

Larsen, M, M. Eriksson, X. Descombes, G. Perrin, T. Brandberg, and F. A. Gougeon. 2011. Comparison of six individual tree crown detection algorithms evaluated under varying forest conditions. *International Journal of Remote Sensing* 32(20): 5827-5852.

Lee, J. S. 1983. Digital image smoothing and the sigma filter. *Computer Vision, Graphics, and Image Processing* 24(2), 255-269.

Martinez, Jean-Michel and Thuy Le Toan. 2007. Mapping of flood dynamics and spatial distribution of vegetation in the Amazon floodplain using multitemporal SAR data. Remote Sensing of Environment 108:209-223.

McGrath, David G., Oriana T. Almeida, Frank D. Merry. 2007. The Influence of Community Management Agreements on Household Economic Strategies: Cattle Grazing and Fishing Agreements on the Lower Amazon Floodplain. International Journal of the Commons 1(1): 67-87.

Melack, J. M. and L. L. Hess. 2009. Remote sensing of the Distribution and Extent of Wetlands in the Amazon Basin. In Amazonian Floodplain Forests: Ecophysiology, Biodiversity and Sustainable Management, Ecological Studies 210: 43-59.

Mertes, L. A. K., D. L. Daniel, J. M. Melack, B. Nelson, L. A. Martinelli, and B. R. Forsberg. 1995. Spatial patterns of hydrology, geomorphology, and vegetation on the floodplain of the Amazon River in Brazil from a remote sensing perspective. *Geomorphology* 13:215-232.

Myint, S. W., P. Gober, A. Brazel, S. Grossman-Clarke, and Q. Weng. 2011. Per-pixel vs. object-based classification of urban land cover extraction using high spatial resolution imagery. *Remote Sensing of Environment* 115(5), 1145-1161.

Novo, E. M. and Y. E. Shimabukuro. 1997. Identification and mapping of Amazon habitats using a mixing model. *International Journal of Remote Sensing* 18(3):1241-1260.

Peixoto, J. M. A., B. W. Nelson, F. Wittmann. 2009. Spatial and temporal dynamics of river channel migration and vegetation in central Amazonian white-water floodplains by remote-sensing techniques. *Remote Sensing of Environment* 113: 3358-2266.

Piedade, J. T. F., W. Junk, S. A. D'Angelo, F. Wittman, J. Schöngart, K. M. do Nascimento Barbosa, and A. Lopes. 2010. Aquatic herbaceous plants of the Amazon floodplains: state of the art and research needed. *Acta Limnological Brasiliensia,* 22(2): 165-178.

Powell, R. L., D. A. Roberts, P. E. Dennison, and L. L. Hess. 2007. Sub-pixel mapping of urban land cover using multiple endmember spectral mixture analysis: Manaus, Brazil. *Remote Sensing of Environment*, 106(2007), 253-267.

Powell, R. L., Hess, L. L., Silva, T. F., Isherwood, J., & McGrath, D. (2014). Inter- and intra-annual characterization of Amazon floodplain habitats with multiple endmember spectral mixture analysis. Paper presented at the annual meeting of the American Association of Geographers, Tampa, Florida, April 19-25.

Reno, V. F., E. M. L. M. Novo, C. Suemitsu, C. D. Renno, and T. S. Silva. 2011. Assessment of deforestation in the Lower Amazon floodplain using historical Landsat MSS/TM imagery. *Remote Sensing of the Enivronment* 115(12),3446-3456.

Roberts, D. A., M. Gardner, R. Church, S. Ustin, G. Scheer, R. O. Green. 1998. Mapping chaparral in the Santa Monica Mountains using multiple endmember spectral mixture models. *Remote Sensing of Environment* 65(3), 267-279.

Rocchini, D. 2007. Effects of spatial and spectral resolution in estimating ecosystem α-diversity by satellite imagery. *Remote Sensing of Environment* 11(2007), 423-434.

Scoggan, H. J. 1978. *The Flora of Canada*. Ottawa: National Museums of Canada.

Sheikh, P. A.,Merry, F. D., & McGrath, D. G. (2006).Water buffalo and cattle ranching in the Lower Amazon Basin: Comparisons and conflicts. Agricultural Systems, 87, 313–330.

Silva, T. F. 2015. Ecosystem Function in Amazon Floodplain Wetlands: Climate Variability, Landscape Dynamics and Carbon Biogeochemistry. Session proposal submitted to American Geophysical Union 2015 Fall Meeting, 14-18 December, 2015, San Francisco.

Silva, T. S. F., M. P. F. Costa, J. M. Melack. 2010. Spatial and temporal variability of macrophyte cover and productivity in the eastern Amazon floodplain: A remote sensing approach. *Remote Sensing of Environment* 114(9), 1998-2010.

Silva, Thiago S. F., John M. Melack, and Evlyn M. L. M. Novo. 2013. Responses of aquatic macrophyte cover and productivity to flooding variability on the Amazon floodplain. Global Change Biology 19:3379-3389.

Smith, N. 1999. Anthrosols and human carrying capacity in Amazonia. *Annals of the American Association of Geographers* 70:533-566.

Souza, C. J., L. Firestone, L. M. Silva, and D. Roberts. 2003. Mapping forest degradation in the Eastern Amazon from SPOT-4 through spectral mixture models. *Remote Sensing of Environment*, 87(4):494-506.

Strahler, A. H., C. E. Woodcock, and J. A. Smith. 1986. On the Nature of Models in Remote Sensing. *Remote Sensing of Environment* 20(1986):121-139.

United States Geological Survey. 2015. Landsat 4-7 Climate Data Record Surface Reflectance Product Guide, Version 5.5.

Weidner, U. 2008. Contribution to the assessment of segmentation quality for remote sensing applications. *International archives of photogrammetry and remote sensing, XXXVII, part 87, Beijing*, pp. 479-484.

Weng, Q. 2012. Remote sensing of impervious surfaces in the urban areas: Requirements, methods, and trend. *Remote Sensing of Environment*, 117(2012):34-49.

Weng, Q. and X. Hu. 2009. Estimating impervious surfaces from medium spatial resolution imagery using the self-organizing map and multi-layer perceptron neural networks. *Remote Sensing of Environment* 113(2009):2089-2102.

Wittman, F., W., J. Schongart, J. C. Montero, T. Motzer, W. J. Junk, M. T. F. Piedade, H. L. Queirox, and M. Worbes. 2006. Tree species composition and diversity gradients in white-water forests across the Amazon Basin. Journal Biogeography 33(8):1334-1347.

Zhou, W., Troy, A., 2008. An object-oriented approach for analysing and characterizing urban landscape at the parcel level. *International Journal of Remote Sensing* 29 (11), 3119-3135.